2021

Bibliometric Review on Liver and Tumour Segmentation using Deep Learning

Jayant Jagtap
jayant.jagtap@sitpune.edu.in

Aamir Habeeb
aamir.habeeb.btech2018@sitpune.edu.in

Avinash Jha
avinash.jha.btech2018@sitpune.edu.in

Shrey Aggarwal
shrey.aggarwal.btech2018@sitpune.edu.in

Khushi Gupta
khushi.gupta.btech2018@sitpune.edu.in

Bibliometric Review on Liver and Tumour Segmentation using Deep Learning

Jayant Jagtap[1], Khushi Gupta[2], Shrey Aggarwal[3], Avinash Jha[4], Aamir Habib[5]

[1]Department of Electronics and Telecommunication, Symbiosis Institute of Technology (SIT), Symbiosis International (Deemed University), (SIU) Lavale, Pune, Maharashtra, India

Email: jayant.jagtap@sitpune.edu.in

[2]Department of Electronics and Telecommunication, Symbiosis Institute of Technology (SIT), Symbiosis International (Deemed University), (SIU) Lavale, Pune, Maharashtra, India

Email: aamir.habeeb.btech2018@sitpune.edu.in

[3]Department of Electronics and Telecommunication, Symbiosis Institute of Technology (SIT), Symbiosis International (Deemed University), (SIU) Lavale, Pune, Maharashtra, India

Email: avinash.jha.btech2018@sitpune.edu.in

[4]Department of Electronics and Telecommunication, Symbiosis Institute of Technology (SIT), Symbiosis International (Deemed University), (SIU) Lavale, Pune, Maharashtra, India

Email: shrey.aggarwal.btech2018@sitpune.edu.in

[5]Department of Electronics and Telecommunication, Symbiosis Institute of Technology (SIT), Symbiosis International (Deemed University), (SIU) Lavale, Pune, Maharashtra, India

Email: khushi.gupta.btech2018@sitpune.edu.in

ABSTRACT

One of the major organs in the body is liver where tumors occur often. Malignant liver tumors pose a serious hazard to human life and health. Manual segmentation of the liver organ and tumor from computed tomography (CT) scans is difficult, time-consuming, and skewed to the clinician's experience, yet it is essential for hepatic surgical planning. However, due to the following considerations, segmenting liver tumors from computed tomography (CT) images is difficult: In CT pictures, the contrast between the liver tumor and healthy tissues is low, and the boundary is indistinct; the picture of the liver tumor is confusing, with a wide range of size, shape, and location. Since there have been a lot of medical imaging techniques with their own advantages and disadvantages over the years, such as MRI, Ultra-sonography (US), Computed Tomography (CT), so on and so forth, CT is often preferred due to its high sensibility (93 %) and specificity (93 %), where CT is often preferred due to its high specificity (93 %) (100 %).

Keywords: Liver segmentation, Tumour segmentation, MPNET, ADCN, U-Net**,** CT images

1. INTRODUCTION

As we all know, deaths occurring from cancer are second most in the world, World health organization (WHO) data says that this disease is responsible for 10 million deaths in 2020 out of which 632,320 almost 6.3% of the total deaths were caused by liver cancer. In 2022, 41,810 new cases of primary liver cancer and intra-hepatic bile duct cancer will be diagnosed (29,300 men and 11,610 women), with 28,220 people (19,610 men and 9,310 women) dying of primary liver cancer. Liver cancer can be found in greater number in countries like Africa and Southeast Asia accounting for quite a large number that is 600,000 deaths annually.

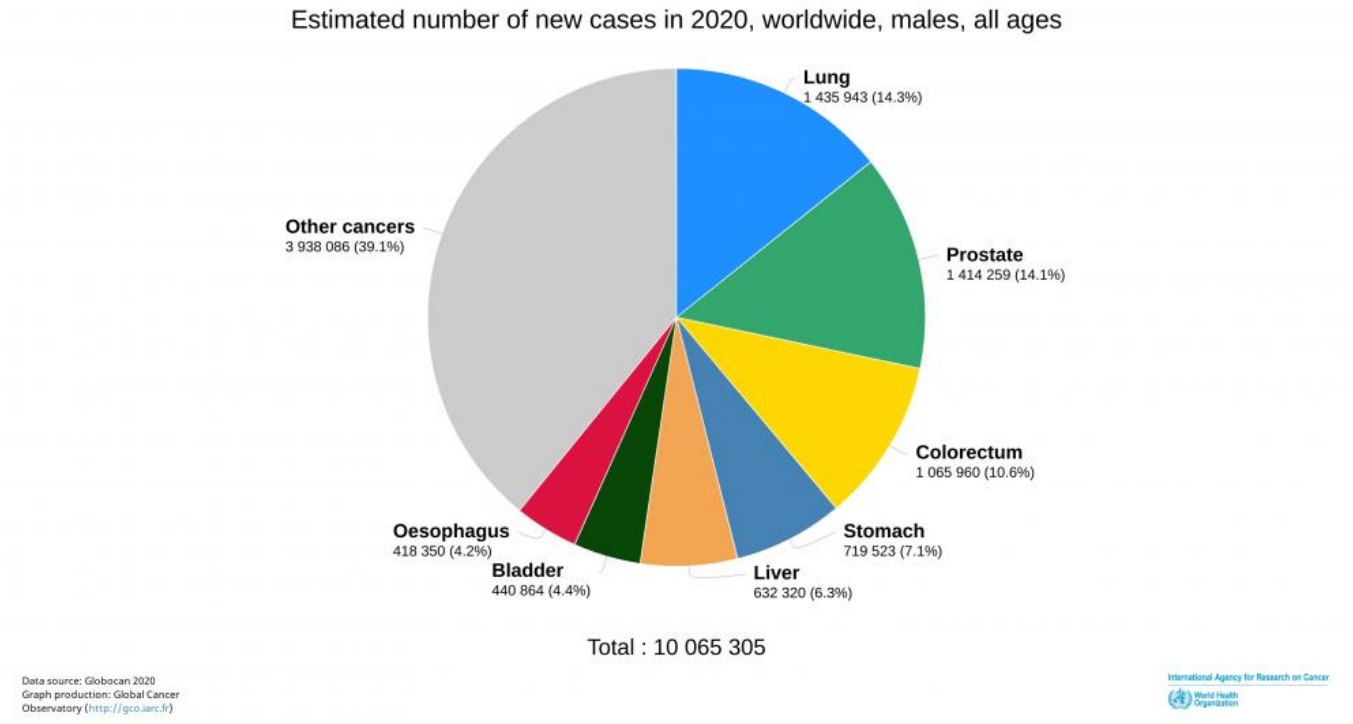

Fig. 1: Deaths due to Cancer [1]

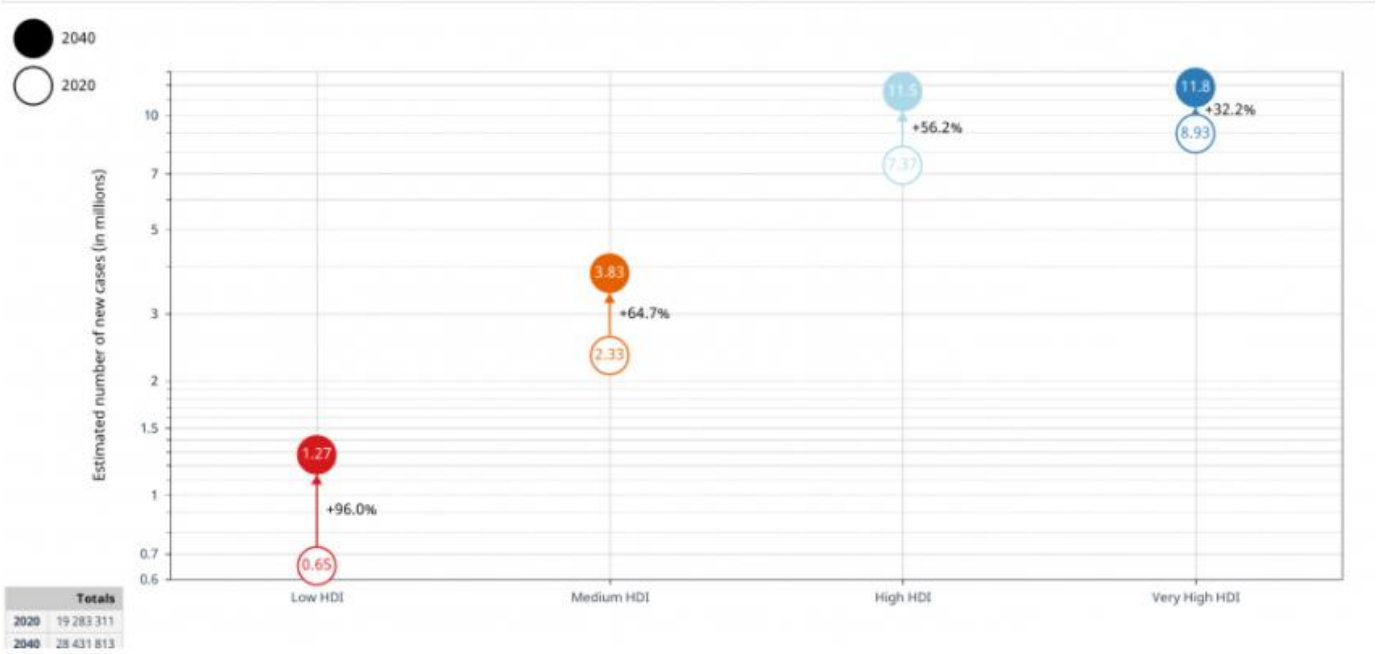

Fig 2: Estimated number of new cases for both the sexes in cancer between 2020-2040, age (0-85+) [2]

The liver is second largest organ in the body. The gallbladder, pancreas, and intestines are all in contact with the liver, which has two lobes: right and left. Because the liver is in contact with so many organs, cancer in the liver is frequently both primary (arising from the many cells that make up the liver) and secondary (resulting from liver metastases) (caused due to cancerous cell from other organs). Among all liver malignancies, hepatocellular carcinoma (HCC) is the most frequent type of primary liver cancer.

The technique of recognising, classifying, and segregating liver and malignant cells from normal non-liver and non-malignant cells in a medical imaging is known as completely automatic liver tumor segmentation. Such methods are generally based on training and testing of large number of labels of liver and tumor from medical image, originally segmented by expert radiologist and doctors. These fully tested and verified techniques can be integrated by developing a software or a Computer Assisted System. Thus, creation of effective and accurate segmentation algorithm for liver and tumor without help from expert radiologist and doctor can save a lot of time, money and life.

2. LITERATURE SEARCH AND DISCUSSION

A large number of researches has been done for liver and tumor segmentation form on semi-automatic, automatic and manual segmentation technique. There is always active participation of expert or doctor required to delineate liver or tumor from medical images in either of manual (with complete involvement) or semi-automatic method (partial involvement). The following sections provides an overview of the related work done in this field:

The researchers created an autonomous approach for segmentation of liver and tumor from CT scans using FCN and three-dimensional dual path multiscale convolutional neural networks (TDPCNN).

FCN- It gets started when a CT scan to segment the liver organ, then trains to predict coarse liver and tumor segmentation, with the localised region-based level seeking to refine the predicted segmentation to discover the correct final segmentation. In TDPCNN the dual path was utilised in the network to balance segmentation performance and computing resource constraints, and at the end of the pathways, the feature maps from both paths were fused.

For liver and tumor segmentation, SSMs, ML classifiers, graph cut, clustering, and other semi/automatic techniques have been proposed.

It is very important to segment tumor for any surgical operation. Accurate and precise location and shape of a tumor are a necessity for better treatment plan at different liver cancer stages. This allows keeping track of the therapy over time.

2.1 Methodology

This report uses a deep learning-based segmentation system to segregate liver and tumors from CT scan pictures. Following are the work's main contributions:

a) It solves the problem of limited data in biological imaging by using data augmentation tasks.
b) We will be decreasing the number of filters in every convolutional layer and hence, it dramatically minimises the amount of time necessary for training of our dataset.
c) It improves algorithm's efficiency in recognising the tumor from CT scans by eliminating slices that contain no data on tumours and use only slices that contain complete information, reducing class imbalance between the tumour and background.

2.2 Publishing Languages

We have used Scopus database in which we used different keywords through which we can find research papers related to our work. Language plays a very important role in analysis for research papers. We found that English is the language in which most of the papers have been published.

Table 1: Language trends in publications

Publication Language	Count
English	508
Chinese	9
German	1
Persian	1
Spanish	1
Total	**520**

Source: http://www.scopus.com

2.2 Publishing outcomes based on keywords

To find the literature surveys of different publications the best way to find them is through keyword-based search. During our research we used the following top keywords present in Table 2 based on our topic.

Table 2: List of keywords

Keywords	Number of Publications
Human	301
Machine learning	272
Article	255
Deep learning	149
Liver cell carcinoma	129
Diseases	114
Liver cancer	93

Source: http://www.scopus.com

2.2 Publication analysis by year

The documents have been collected from year 2012 to 2020 which includes sources such as research papers, thesis, journals, book chapters etc. Table 3 given below shows number of publications done in a particular year. The highest publications were made in 2020 followed by 2019.

Table 3: Publication count per year

Publishing Year	Count
2021	5
2020	209
2019	121
2018	55
2017	43
2016	27
2015	19
2014	23
2013	12
2012	4
Total	518

Source: http://www.scopus.com

2.2.1 Documents with respect to subject area

Liver cancer is purely the medical term. Hence maximum documents are found under medical category (27%). Following to the medical category, computer science (18.5%) and engineering (10.6%) which combinedly covers 29.1% of documents.

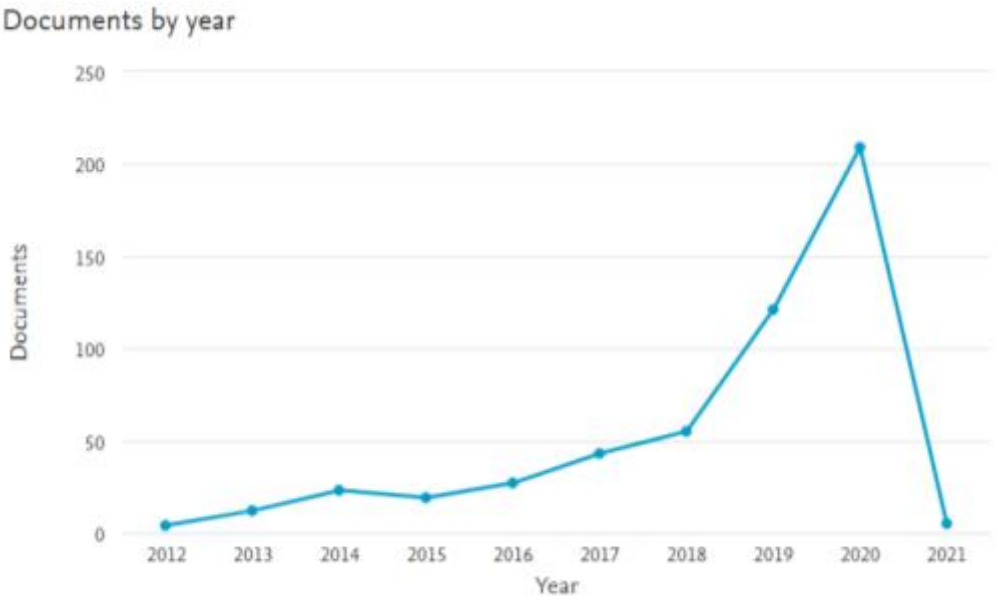

Fig.3: Documents by year
Source: www.scopus.com

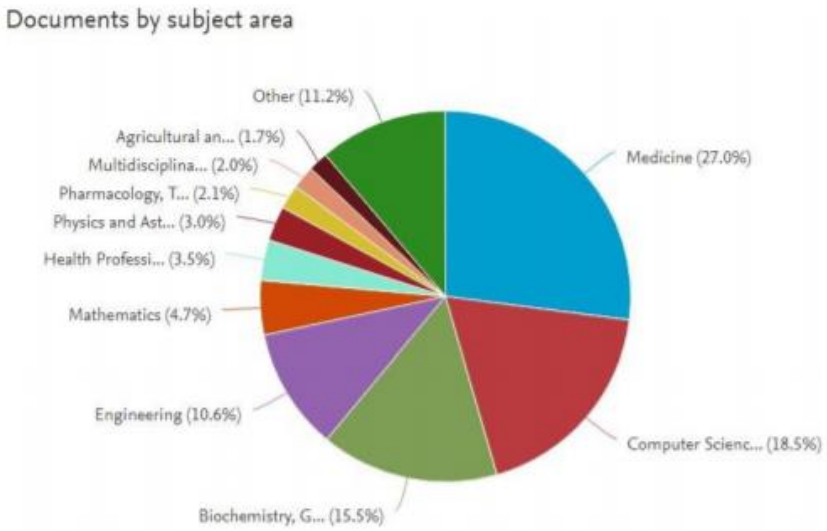

Fig.4: Documents with respect to search area
Source: www.scopus.com

3. ALGORITHM

The shape, size, and contrast of a liver tumor can differ from that of other tumors. If we compare a segment to only one region of interest, we can see that liver tumors can manifest in a variety of ways and frequently lack clearly visible edges. Typically, these things contribute to extra noise while segmenting. As a result, segmenting liver tumors is considered the most challenging task in medical science. The following are the several types of methods for segmenting liver tumors:

3.1 Thresholding methods

Based on our findings, the levels of grey tumors in non-tumor areas differentiate from pixels, which means that thresholds can be a simple yet efficient technique for automatic distinction between the tumor and the liver and the background. By generating an adequate threshold value using histogram analysis, maximizing variance between classes, and iteratively setting the threshold value using an isodata algorithm, threshold-based methods have improved tumor segmentation results.

3.2 Spatial regularization methods

Prior imaging or morphology information, such as tumor size, shape, surface, or geographical information, is used in spatial regulatory systems. This data is used to impose restrictions such as regularization and penalization. Adaptive thresholding approaches are widely used in lesion segmentation.

3.3 Using supervised classification and unsupervised clustering algorithms on local picture characteristics

Because of the varied incidence of liver tumors, ML-based approaches are significantly established in liver tumor segmentation tasks. K-means and fuzzy c-means clustering, as well as deformable models for segmentation refinement, are examples of clustering algorithms. SVM [4][6] in combination with AdaBoost trained on texture features and image intensity profiles, logistic regression, and RF recursively decomposing super voxels are among the supervised classification methods. (A voxel is a single image, or data point, on a three-dimensional grid with regular spacing. This piece of data can contain a single piece of information, such as opacity, or multiple pieces of information, such as color in addition to opacity.)

3.4 Deep Learning Techniques

Prior to LiTS, deep learning techniques for liver tumor segmentation were rarely applied. For liver and tumor segmentation, one method used an eleven-layer 3D CNN for segmentation refinement after cascading 3D CNNs [4].

4. METHODS FOR SEGMENTATION

4.1 The cascaded framework

Fig.5 depicts the cascade system for segmentation of tumor and liver. In this scenario, two layers are employed to segment liver and the tumor. The MPNet first separates liver from the 3-D CT images of the abdomen, allowing us to get an accurate liver area. The liver is then utilized as the ACDN's bounding box, and the network's input images are cropped to train it for tumor segmentation. Two steps in the network development process are training the network for weight update and segmentation utilizing the recording network. The bounding boxes containing the liver are results of the segmentation of the liver, whereas the bounding box containing tumor are directly selected from the bottom truth during training to find out the ideal network parameters for liver or tumor.

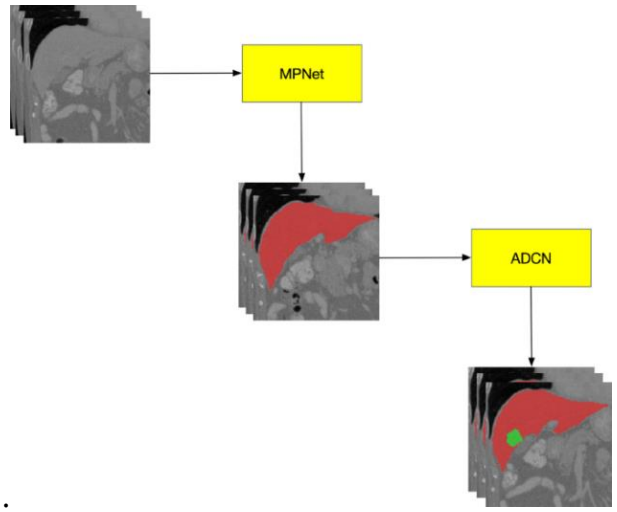

Fig.5: Cascaded framework for Segmentation [3]

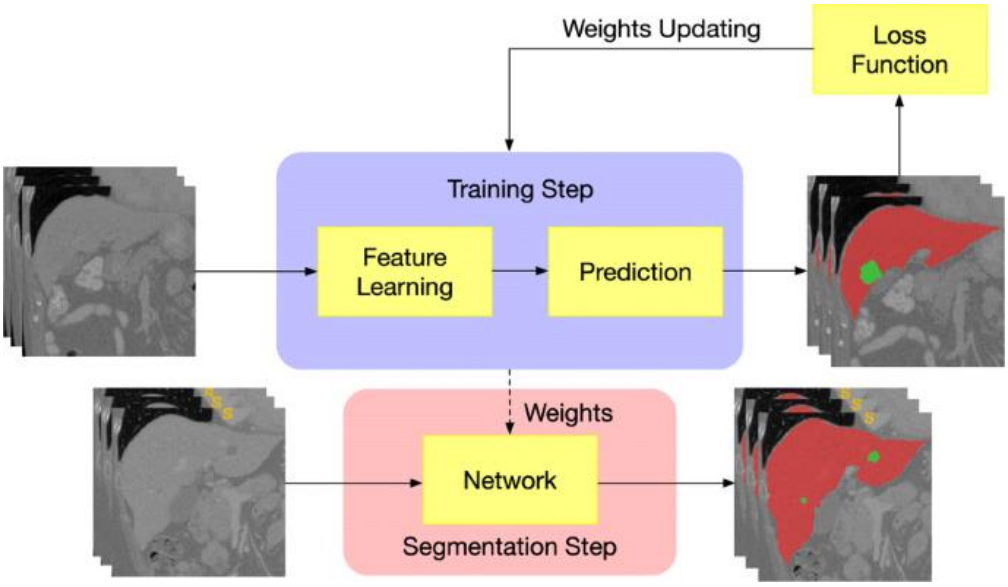

Fig.6: The training and segmentation part from the construction of network [3]

4.2 Multi-plane integrated fully convolutional networks used for liver segmentation

An FCN's (fully convolutional network) output is the same size as its input. For each voxel it receives as input, FCN can build a score map. MPNet's core technique is to train data from the input 3D CT volumes in three planes that are axial, sagittal, and coronal. To obtain the final segmentation results, we need to apply the multi-plane integration methodology to find the joint predictions of three networks during the segmentation step.

4.3 Adversarial densely connected network for tumor segmentation

The obtained ROI will be fed into the tumor segmentation network. Because of its demonstrated performance in image segmentation, we seek to optimize the convolutional encoder-decoder structure for the purpose of liver tumor segmentation. For tumor voxel classification, this method uses a hostile densely connected network using a hostile training method, dense connection, dilated convolution, and multi-scale feature fusion technology. Here, in the ADCN architecture that can be seen in Fig. 7. The MPNet provides the input for ADCN, which is clearly 3D Computed Tomography liver volumes, and the output is a map that displays a probability map showing how the voxels belong to tumor.

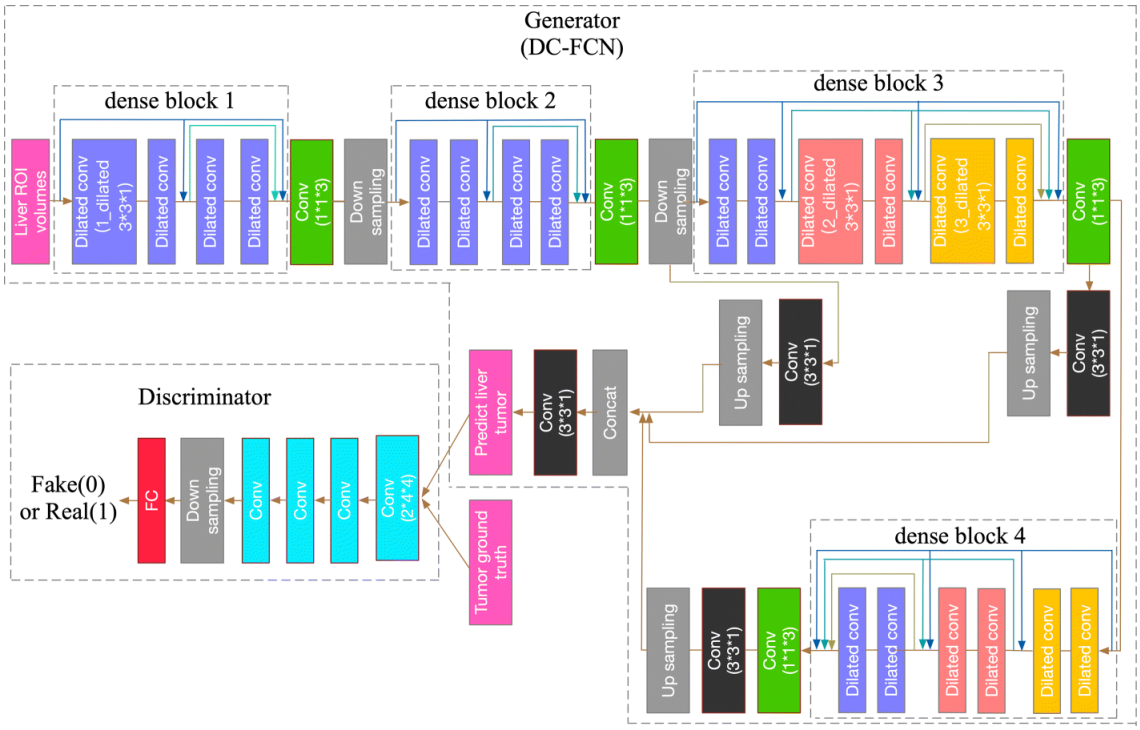

Fig.7: The Structure of ADCN

4.4 UNET Architecture and Training

Olaf Ranneberger was the first to develop the UNET architecture for Bio Medical Image Segmentation. There are two ways in the architecture. The first path is the contraction path (also known as the encoder), which is used to record the image's context. The encoder is just a typical convolutional and max pooling layer stack. The symmetric expanding path (also known as the decoder) is the second path, which is used to provide exact localization via transposed convolutions. As a consequence, it's an end-to-end FCN, it means it has just Convolutional layers and no Dense layers, and can accept any image (of any size). The following is a diagram of the U-Net architecture in its most general version.

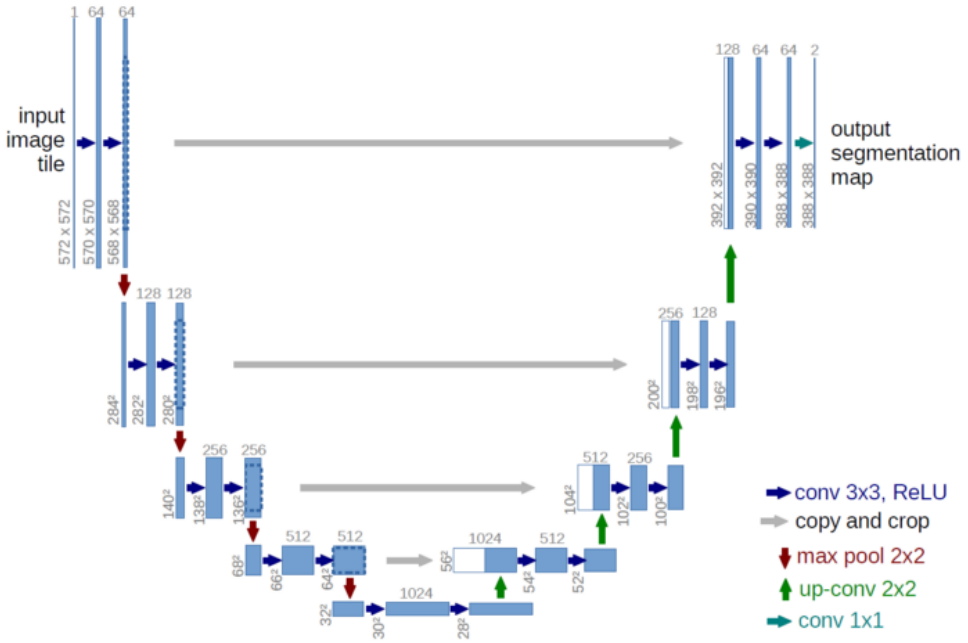

Fig.8: U-net architecture particularly said to be multi-channel feature [13]

4.5 Accuracy of different methods:

Table 4: Evaluation results of different methods (for tumor segmentation) [15]

Methods	ACC	IoU	DSC	AUC
U-Net	0.92	0.53	0.65	0.73
ResNet	0.98	0.62	0.67	0.77
C-UNet	0.99	0.67	0.67	0.87

Three mainly used methods for image tumor segmentation are U-Net, C-UNet, and ResNet [15]. These three methods were selected for comparison of tumor segmentation capability. Table 4 tabulates the tumor extraction results of all the methods in terms of accuracy, intersection over union (IOU), dice similarity coefficient (DSC), and area under curve AUC. In accuracy that is ACC, all methods achieved values above 0.9 due to the fact that both positive (tumor) and negative (background) samples were counted in ACC. Thus, ACC is not an ideal metric for segmentation where the positive and negative samples are unbalanced [15]. On the opposite hand, IoU, DSC, and AUC were better metrics for the segmentation task.

Table 5: Evaluation results of different methods (Liver Segmentation) [4]

Methods	DSC	VOE	RAVD	ASD (mm)	MSD (mm)
RF Classifier	99.03	0.44	1.96	0.529	3.703
SVM Classifier	96.79	2.12	10.11	3.29	25.76
DNN Classifier	97.11	1.89	8.67	2.98	24.04

Three proposed methods for liver segmentation are RF, SVM and DNN [4]. Table 5 shows that the RF classifier is the clear winner in terms of Dice similarity coefficient, which is crucial in the Accuracy section. But in our thesis, we will be using the 2nd most used method that is DNN as other that DSC it also has many other features and with good datasets the accuracy can be increased.

5. AVAILABLE DATASETS

Table 6: Available datasets and information about them [6]

Dataset	Institution	Liver	Tumor	Volumes	Modality
3D-IRCADb-01	IRCADb	Yes	Yes	20	CT
3d-IRCADb-02	IRCADb	Yes	Yes	2	CT
LiTS 2017		Yes	Yes	131	CT
TCGA-LIHC	TCIA	Yes	Yes	1688	CT, MR, PT
MIDAS	IMAR	Yes	Yes	4	CT

Table 6 shows the list of available datasets and if they provide us with liver and tumor segmentation and if yes then the volume is also mentioned in the table.

5.1 Datasets we are considering for use

5.1.1 3DIRCADb:

The 3D-IRCADb is a database that contains hidden medical related photographs [1][4][15], as well as various segmented structures that are useful to our project, all of which are human-made and performed by medical specialists. Three-dimensional CT scans of liver tumors in ten women and 10 men are included in the database. The slice spacing can be anywhere between 1.6 and 4.0 mm, while the in-plane resolution can be anywhere between 0.57 and 0.87 mm. In this dataset, the scans are performed with the arterial phase in the inhaled position. The training set consisted of 10 scans, the validation set consisted of five scans, and the test set consisted of five scans.

5.2.2 LiTS:

The LiTS dataset includes 201 three dimensional abdominal CT scans with a resolution of 512×512 per slice with liver and tumor region segmentation labels [1][2][3]. The slice spacing varies ranging from 0.45-5.0 mm, and the in-plane resolution varies in range of 0.60-0.98 mm. We clipped the intensity values to the range [300, 400] HU and normalised the images to [0, 1] to remove extraneous features. The LiTS 2017 dataset had 131 scans, divided into 102 scans for training, 20 scans for verification, and 9 scans are used for testing.

5.2 Reasons for choosing the dataset

When comparing the model trained with 512×512 resolution data to the model trained with low resolution data, we discovered that the model trained with 512×512 resolution data improves segmentation results by about 2% for the liver and 7% for a tumor. Down sampling has a more detrimental impact on tumour segmentation tasks with a lower objective. As a result, we have to test and train models using data with 512×512 resolution, and accuracy will be substantially higher because both datasets have the same resolution.

Table 7: Summary of the datasets trained with numerous data [6]

Category	Datasets	Resolutions	Dice Similarity Coefficient (DSC)
Liver		512*512	0.953
	LiTS 2017	256*256	0.947
		128*128	0.936
		512*512	0.929
	3D-IRCADb	256*256	0.924
		128*128	0.91
Tumor		512*512	0.699
	LiTS 2017	256*256	0.655
		128*128	0.615
		512*512	0.623
	3D-IRCADb	256*256	0.597
		128*128	0.567

In Table 7 as we can see that LiTS has the better Dice similarity coefficient as compared to 3D-IRCADb for both liver and tumor segmentation.

Table 8: A summary of the results performed on LiTS 2017 and 3D-IRCADb [6]

Category	Dataset	Function loss	DSC	95th Percentile of the Hausdorff Distance Metrix (HD95) (mm)	Average Symmetric Distance (ASD)(mm)	TNR	TPR
Liver	LiTS 2017	L_{Reg}	0.953	5.44	1.61	0.957	0.998
		L_{hd}	0.962	3.60	1.05	0.971	0.998
		L_{bd}	0.963	4.24	0.88	0.973	0.999
		L_{sdm}	0.966	3.23	1.07	0.982	0.999
	3D-IRCADb	L_{reg}	0.929	8.74	2.58	0.921	0.997
		L_{hd}	0.942	6.97	2.17	0.949	0.998
		L_{bd}	0.947	4.15	1.87	0.955	0.998
		L_{sdm}	0.948	4.68	1.81	0.958	0.998
Tumor	LiTS 2017	L_{reg}	0.699	9.36	2.17	0.655	0.998
		L_{hd}	0.731	8.77	1.82	0.682	0.998
		L_{bd}	0.745	8.14	1.68	0.708	0.999
		L_{sdm}	0.764	6.72	1.26	0.761	0.999
	3D-	L_{Reg}	0.623	13.46	3.72	0.564	0.999

	IRCADb	L_{hd}	0.648	11.25	3.08	0.587	0.999
		L_{bd}	0.677	9.88	2.88	0.674	0.999
		L_{sdm}	0.682	9.47	2.82	0.654	0.999

Table 8 shows the summary of the two datasets mainly on the factors like Hausdorff Distance Matrices the less it the more will be the accuracy. Then on the basis of ASD, True Negative and Positive Rate. In all of the above parameters the LiTS database is outshining the 3D-IRCADb database.

5.3 Dataset extraction:

The datasets can be downloaded from Kaggle. In the dataset .nii files are used for 3-D imaging. Therefore, we will be converting those 3D images into 2D images using U-Net architecture (python code).

6. GENERALIZED BLOCK DIAGRAM AND WORKING

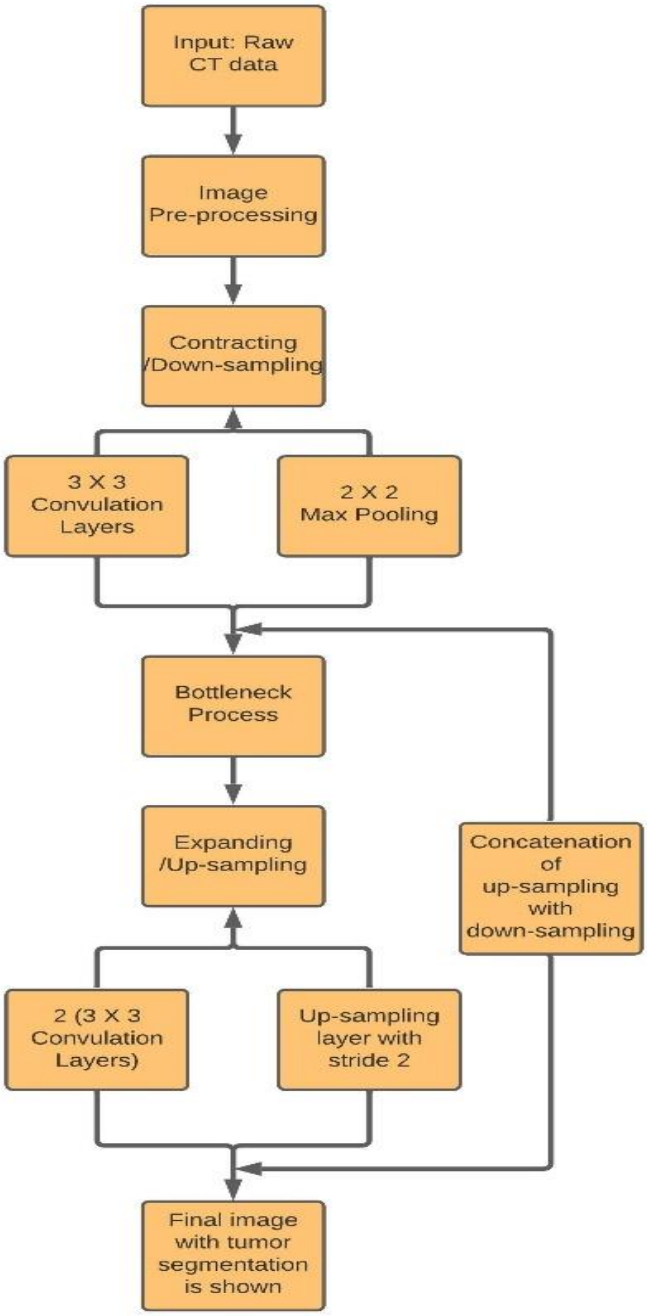

Fig.9: Generalized block diagram for liver and tumor segmentation

1. The user will input the CT scan of the liver into the database. the image will be gone through filtering and normalizing.
2. The picture will go through the process of image segmentation and will follow a segmentation algorithm the algorithm is based on the UNet architecture. This algorithm includes two 2D UNet architectures / TDP-CNN architecture, for the liver and its tumor. These architectures were designed to segment liver and tumor from the abdominal CT scan images.
3. Both liver and the tumor are segmented using a U-net architecture. It has a contracting path, an expanded way, and a bottleneck component, just like the original U-Net.
4. **Contraction and down sampling:** ReLU Normalization and activation functions are necessary. This contraction path captures the context or semantics of the input image in order to execute segmentation. Using convolutional and pooling layers, it recovers features that provide information about what is in an image.
   a) Consists of Convolution Layer with ReLU
   b) Consists of Max Pooling later
5. **Bottleneck:** Between the contracting and extending paths is this section of the network. Two convolutional layers with batch normalisation form the bottleneck.
6. **Expanding or Upsampling Path:** Four bricks make up the decoder, or expanding path. Up-convolution layers are often used to restore the feature map size and offer spatial information to the segmentation image in all of these blocks.
   a) With stride two, add an up convolution or deconvolution layer.
   b) The cropped feature map from the contracting path is joined with matching cropped feature map.
   c) Two 3 by 3 Convolution layers with activation function are included. Here ReLU is used for activation.

7. DEEP LEARNING NETWORK WITH ReLU FUNCTION

In deep learning, the deep network is taught to recognise qualities by gathering and recombining information from previous levels. This capability is referred to as feature hierarchy that provides the deep-learning network with the ability to handle very large high-dimensional data which has billions of parameters passing the nonlinear function. DNN can be used for both automatic feature extraction and feature classification. In our thesis, we have used deep-learning networks in a supervised mode as a binary classifier. The DNN classifier had three hidden layers (as shown in Fig.10). For each of the three layers, the ReLU activation function is used as an activation function for non-linearity. An activation function outputs a nonlinear transformation of the weighted data, which is the product of input data and weights. Where, X is the input neuron matrix, Bi is bias, and Wi is 40-weight matrix for layer I in ReLU, then the output from layer is provided through equation (1).

$$Z_i = \mathrm{ReLU}(XW_i + B_i) = \max(0, XW_i + B_i) \qquad (1)$$

where layer i is ranging from 1 to total number of output and hidden layers.

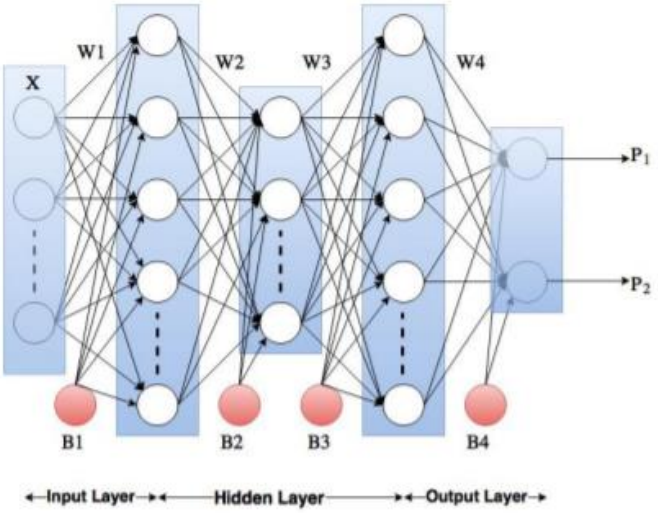

Fig.10: Binary DNN Classifier architecture [4]

7.1 Method for implementing binary DNN classifier

1. First, an NN network with input layer, three hidden-layers, and output layer was defined. The input and output layers were assigned twenty-six and two nodes respectively. The first, second, and third hidden layers were assigned twenty, thirty, and fifteen nodes respectively.

2. The network was then provided with random initial weight and bias values for each neuron in the network. The weight with ReLU activation function for all neurons was initialized using equation (2).

$$w = \text{random}(n) * \sqrt{n/2} \qquad (2)$$

where n is the number of inputs, and random () is a function that randomly samples value from zero mean and unit standard deviation. Because every neuron in the network computes the same output, they will all calculate the same gradients throughout back-propagation to modify the same parameter, leading in no asymmetry. Small random values from a uniform distribution are also insufficient, as the output from a randomly initialised neuron grows as the number of inputs increases.

Therefore, the variance was normalized as shown in equation (2). The bias values were initialized using the same formula replacing weight with bias in the equation (2).

3. The ReLU activation function was used in each neuron as a trigger to obtain and propagate some gradient.

4. Let us consider X as an input matrix, W as weight matrix, and B as the bias matrix, then the output at each neuron was derived in the form of a matrix as equation (3).

$$Y = W X + B \qquad (3)$$

The final output of each neuron was calculated using the ReLU function as max (0, Y).

5. The next step is regularization to prevent overfitting. we have used L2 regularization which is implemented by adding ½ λw^2 term for every weight w in the network to the output. $\lambda > 0$ is a non-negative hyperparameter termed as regularization strength, and $w \in W$ for every weight in the network.

6. The next step involves calculating the loss function. In this thesis, we have used cross-entropy function (C) which in the binary case is given by equation (4).

$$C = -\frac{1}{N}\sum_{n=1}^{N}[y_n \log p_n + (1 - y_n)\log(1 - p_n)] + \frac{\lambda}{2}\|W\|_2^2 \qquad (4)$$

7. Next, the weights of each neuron were updated based on the loss function using the back propagation method with Stochastic Gradient Descent (SGD) (discussed in detail in the next subsection of this chapter).

8. Finally, the process was repeated for the least error value. The weights and other parameters were saved from the trained DNN classifier to predict test data.

8. SOFTWARE REQUIREMENT

The datasets can be acquired from programming platforms like Kaggle and python 3 notebooks in anaconda for the major coding part.

LiTS and 3D-IRCAD datasets were utilized in this paper.

9. PERFORMANCE AND ACCURACY PARAMETERS

9.1 Parameters for performance evaluation

To perform a comparison of various algorithms proposed in our research paper, it is very important to measure and correctly evaluate the performance of segmentation algorithm along with classifiers as there are many lives depended on this. Therefore, we have used aforementioned parameters that are widely used in the field of ML and medical image processing [4]. Discussion about the definitions and different methods on how to increase accuracy and give suitable results are mentioned in the above sections.

9.1.1 Quality measures for individual classifiers

There are mainly three cases on which we measure our quality for individual classifiers those are AC, SN and SP [4]. The calculations for these parameters are based on confusion matrices. As the binary classifier takes all the instances present in the dataset into consideration it can be further predicted in the four following cases:

1. **True Positive (TP):** It is the correct positive prediction. let us consider 0 as positive class and 1 as negative class, then all those values that classifier predicts as zero which confirms with its desired value (true labels) are true positive value. we found the sum of such values.

2. **False Positive (FP):** The incorrectly predicted positive values are FPs. FPs are all those values which are predicted as 0 but have 1 as the desired value.

3. **True Negative (TN):** TN values refer to those values which are correctly predicted as negative. In this case, both predicted and desired value are 1.

4. **False Negative (FN):** The value correctly predicted as negative refer to FN. For FN, the desired value is 0, but the classifier incorrectly predicts negative class or 1.

The cases above can further be classified into a confusion matrix shown in the Fig.11.

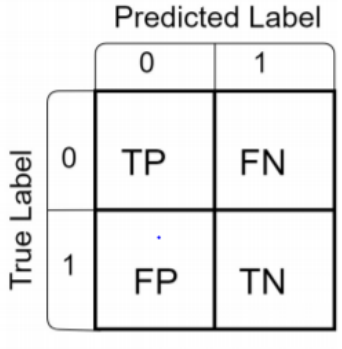

Fig.11: Confusion Matrix

Based on the four outcomes that are possible for binary classifier mentioned in confusion matrix AC, SN, and SP can be defined as follows:

1. **Accuracy (AC):** AC is the ratio of total number of correct predictions to the total number of data present in the dataset. The total number of all correct predictions is the sum of TN and TP value, so the formula for AC can be expressed as equation (5).

$$AC = \frac{TP+TN}{P+N} \qquad (5)$$

Here, P refers to all the positive values and N refers to all the negative values. The best value for AC is said to be as 1 and the worst value is 0

2. **Sensitivity (SN):** SN is calculated as the ratio of a total number of correct positive predictions to a total number of positive. SN is also sometimes referred to as Recall or True Positive Rate (TPR). SN can be expressed as equation (6).

$$SN = \frac{TP}{TP+FN} = \frac{TP}{P} \qquad (6)$$

Here, the best value for sensitivity is 1 and the worst value can be said as 0.

3. **Specificity (SP):** SP is also referred to as True Negative Rate (TNR), and equation (7) is used for calculation.

$$SP = \frac{TN}{TN+FP} = \frac{TN}{N} \qquad (7)$$

10. CONCLUSION AND FUTURE WORK

10.1 Future Work

Based on a high value of classifier accuracy, the idea can be implemented and tested over a wide variety of dataset as it has succeeded for this particular set of raw images. Moreover, the technique used in this research paper does not require any postprocessing to refine the output since we are using a U-net architecture that provides us with an output that has same dimensions and quality as the input. In future, a large number of a dataset can be added to perform analysis provided enough processing speed.

Further we can use this similar project in kidney, lungs, brain, etc., and for different medical image formats MRI, ultrasound, etc.

10.2 Conclusion

Segmentations obtained by the abdominal CT scan image is a key task for many clinical applications in medical sciences. Automatic methods for such problem are of the great essence as they reduce time, effort, provide quality assistance to experts as well as early determination and diagnosis of the tumor. To be of practical use, such application of segmenting liver area and tumor area should be very accurate, precise, and verified using metrics popular in medical image processing in order that a radiologist can perform segmentation quickly without help from technician. The segmentation is a very challenging work because of the complexity of liver surface, variation in liver and tumor size throughout the CT image slices, ambiguity in boundaries of alike intensity tissues and nearby organs. Many types of research and works have been done previously to develop an automatic and semi-automatic method for liver and tumor segmentation. But there are only a couple of methods that do the segmentation of both liver and tumor using the same technique or single approach and provides better and accurate result. Most of the method used practically in clinical applications are the semi-automatic method which requires more or less user interaction for initial contour defining or parameter adjustments, etc. The methods thus far that has been developed on previous work are mostly based on statistical method. The drawbacks of such methods are a lot of research work requirement in statistics, and the process of determining information on statistics are very sensitive. Such statistical

model and most of the other approach aforementioned requires more research for expansion to some other organs or tissues.

The proposed general segmentation algorithm is the latest concept based on training texture features using machine learning algorithm. Texture features are more informative than most of the other features, and the use of machine learning algorithm is in every application with its influence and application to be more increased in future. We took the concept and applied it within the medical field for liver and tumor segmentation with Gabor feature and three different machine learning algorithms.

In this research paper, we have used 3D-IRCADb dataset which is a verified resource from Institute of France for surgical planning and is publicly available to conduct research which shows the authenticity of data. For the individual classifier and segmentation algorithm, we additionally employed forenamed metrics to demonstrate the suggested method's good performance. The proposed method implementation also provides a perspective for this method to be practically used with some improvements on an equivalent fundamental.

REFERENCES

[1] https://www.uicc.org/sites/main/files/thumbnails/image/Men%27s%20cancer%202020.png

[2] https://www.uicc.org/news/globocan-2020-new-global-cancer-data#:~:text=IARC%20released%20on%2014th%20December,million%20cancer%20deaths%20in%202020.

[3] Lu Meng, Yaoyu Tian, Siang Bu, "Liver and tumor segmentation based on 3-D convolutional neural network and dual scale," *Journal of Applied Clinical Medical Physics*, vol. 21, 2019, doi: 10.1002/acm2.12784.

[4] Yodit Abebe, Dr. Kinde Anlay, Mohammed Aliy, "Deep Learning based Liver Cancer Segmentation from Computed Tomography Images," *Research Square*, 2020, doi: 10.21203/rs.3.rs-65573/v1

[5] Omar Ibrahim Alirr, "Deep learning and level set approach for liver and tumor segmentation from CT scans," *Journal of Applied Clinical Medical Physics*, vol.21, 2020, doi: 10.1002/acm2.13003.

[6] Ujjwala Shrestha, "Automatic Liver and Tumor Segmentation from CT Scan Images using Gabor Feature and Machine Learning Algorithms," *University of Toledo*, 2018.

[7] Syed M.S. Reza, Dara Bradley BS, Nina Aiosa BS, Marcelo Castro, "Deep Learning for Automated Liver Segmentation to Aid in the Study of Infectious Diseases in Nonhuman Primates,"

[8] Sultan Almotairi, Ghada Kareem, Mohamed Aouf, Badr Almutairi, and Mohammed A.-M. Salem, "Liver Tumor Segmentation in CT Scans Using Modified SegNet,", *Sensors*, 2020, vol. 20, doi: 10.3390/s20051516.

[9] https://www.ircad.fr/research/3dircadb/

[10] Kiran Malhari Napte Mr, Anurag Mahajan Dr., "Liver Segmentation and Liver Cancer Detection Based on Deep Convolutional Neural Convolutional Neural Network: A Brief Bibliometric Sur al Network," *Library philosophy and practice*,2020.

[11] Lu, F., Wu, F., Hu, P., Peng, Z. & Kong, D. (2017), "Automatic 3D liver location and segmentation via convolutional neural network and graph cut," *International Journal of Computer Assisted Radiology and Surgery*, vol. 171-182.

[12] P. Campadelli, E. Casiraghi and A. Esposito, (2009)' "Liver Segmentation from Computed Tomography Scans: A Survey and a New Algorithm. Artificial Intelligence in Medicine," 45(3), vol. 185-196.

[13] Hasan Faraz Khan, "Building U-Net architecture for biomedical image segmentation".

[14] Weiwei Wu, Shuicai Wu, Zhuhuang Zhou, Rui Zhang, and Yanhua Zhang, "3D Liver Tumor Segmentation in CT Images Using Improved Fuzzy *C*-Means and Graph Cuts," *BioMed Research International*, vol.2017, 2017, doi: 10.1155/2017/5207685.

[15] Wen-Fan Chen, Hsin-You Ou, Keng-Hao Liu, Zhi-Yun Li, Chien-Chang Liao, Shao-Yu Wang, Wen Huang Yu-Fan Cheng and Cheng-Tang Pan, "In-Series U-Net Network to 3D Tumor Image Reconstruction for Liver Hepatocellular Carcinoma Recognition," *MDPI AG*, vol. 11, 2020, doi: 10.3390/diagnostics11010011